The AAPS Journal (© 2017)
DOI: 10.1208/s12248-016-0043-7

Research Article

Radiomitigation and Tissue Repair Activity of Systemically Administered Therapeutic Peptide TP508 Is Enhanced by PEGylation

Scott D. McVicar,[1,3] Kempaiah Rayavara,[2] and Darrell H. Carney[1,2]

Received 10 October 2016; accepted 30 December 2016

Abstract. TP508 is a synthetically derived tissue repair peptide that has previously demonstrated safety and potential efficacy in phase I/II clinical trials for the treatment of diabetic foot ulcers. Recent studies show that a single injection of TP508 administered 24 h after irradiation significantly increases survival and delays mortality in murine models of acute radiation mortality. Thus, TP508 is being developed as a potential nuclear countermeasure. Because of the short plasma half-life of TP508, we hypothesize that increasing the peptide bioavailability would increase TP508 efficacy or reduce the dosage required for therapeutic effects. We, therefore, evaluated the covalent attachment of various sizes of polyethylene glycol to TP508 at either its N-terminus or at an internal cysteine. A size-dependent increase in TP508 plasma half-life due to PEGylation was observed in blood samples from male CD-1 mice using fluorescently labeled TP508 and PEGylated TP508 derivatives. Biological activity of PEGylated TP508 derivatives was evaluated using a combination of biologically relevant assays for wound closure, angiogenesis, and DNA repair. PEG5k-TP508 enhanced wound closure after irradiation and enhanced angiogenic sprouting in murine aortic ring segments relative to equimolar dosages of TP508 without enhancing circulating half-life. PEG30k-TP508 extended the plasma half-life by approximately 19-fold while also showing enhanced biological activity. Intermediate-sized PEGylated TP508 derivatives had enhanced plasma half-life but were not active *in vivo*. Thus, increased half-life does not necessarily correlate with increased biological activity. Nevertheless, these results identify two candidates, PEG5k-TP508 and PEG30k-TP508, for potential development as second-generation TP508 injectable drugs.

KEY WORDS: drug development; peptide conjugation; radiomitigation; tissue repair.

INTRODUCTION

TP508 is a synthetically derived peptide with potent tissue repair properties. The 23 amino acid sequence of TP508 (AGYKPDEGKRGDACEGSDGGPFV-NH2) is identical to that of residues 508–530 of human prothrombin (1). Originally identified as a peptide sequence capable of specifically competing for thrombin binding sites on fibroblasts, it was discovered that this peptide could stimulate anti-inflammatory effects of thrombin without thrombin's serine protease and coagulation activity (1). Since then, investigations have shown that TP508 stimulates diverse wound healing effects including acceleration of angiogenesis (2,3), enhancement of osteogenesis (4), induction of vascular endothelial nitric oxide signaling (5), and enhanced proliferation of stem cells (6). These activities have been shown in various animal models to reduce time to full-thickness dermal wound closure (2,7–9), accelerate bone fracture repair (10–13), and attenuate damage from myocardial ischemic reperfusion injury and chronic ischemia in both normal and diabetic models (14–17). It has also been determined that the sequence of TP508 remains intact within an 11-kDa C-terminal major fragment of thrombin that is released when fibrin clots are broken down by neutrophil elastase (18). This suggests that TP508 may represent the minimal peptide sequence necessary for mimicking a signaling molecule that naturally occurs at the late inflammation/early proliferation stage of wound healing.

As an investigational drug product, TP508 (also known as rusalatide acetate, CAS no. 87455-82-6, and by the brand name Chrysalin®) has demonstrated safety and potential efficacy in clinical trials for two indications. In a double-blinded, placebo-controlled phase I/II clinical trial for accelerating closure of diabetic foot ulcers, 10 μg doses of TP508 applied twice weekly to the affected area reduced time to

[1] Department of Biochemistry and Molecular Biology, The University of Texas Medical Branch, 301 University Blvd., Galveston, Texas 77555, USA.
[2] Chrysalis BioTherapeutics, Inc., Galveston, Texas, USA.
[3] To whom correspondence should be addressed. (e-mail: sdmcvica@utmb.edu)

Published online: 17 January 2017

closure by 40% and increased total closure of the ulcers by 72% over placebo (9,19). In phase II and phase III clinical trials, TP508 accelerated radiographic healing of distal radius fractures, but in the phase III trial, the primary endpoint of reducing time to cast or fixation removal was only met in osteopenic subjects (9,10). During these trials, approximately 600 patients had TP508 administered with no adverse events.

Recent preclinical investigations demonstrate that TP508 also counteracts the effects of radiation exposure, possessing both radioprotective and radiomitigating properties (20,21). This suggests that TP508 may be used a nuclear countermeasure and to prevent radiation therapy damage to normal tissue (22,23). For these indications, TP508 efficacy is greatest when administered as a systemic injection. This represents a new route of administration for TP508 since the diabetic foot ulcer clinical trial used a topical application of TP508 and the distal radius fracture repair trial used local injection into the fracture site. It is anticipated that the therapeutic efficacy of TP508 *via* systemic administration may be limited by its short plasma half-life of approximately 14 min (15). This is a common challenge for small protein therapeutics. Thus, a substantial amount of research has been done to find ways to enhance the pharmacokinetic bioavailability of polypeptide drugs. These include cyclization (24,25), creation of chimeric proteins and antibody drug conjugates (26,27), and attachment to biocompatible polymers (28–31). This research provides a drug development opportunity to improve the therapeutic efficacy of TP508 systemic administration by covalently modifying the peptide for enhanced plasma half-life. We chose to examine TP508 covalently attached to various lengths of polyethylene glycol (PEG) at the peptide N-terminus to determine whether any of the derivatives displayed increased plasma half-life while maintaining TP508's biological activity (Fig. 1). Since TP508 naturally forms a biologically active homodimer by creating a disulfide bridge between the Cys14 residues at neutral pH (14), we also theorized that covalent attachment of PEG to the Cys14 residue of TP508 *via* a maleimide linkage might retain biological activity. C-terminal attachment constructs were not examined, as previous studies suggest that C-terminal modifications of TP508 result in a loss of activity (unpublished data). These peptides were prepared using fresh solid-phase peptide synthesis at the American Peptide Company (Sunnyvale, CA). These peptides had a minimum of 95% purity by SDS-PAGE (Fig. 2a), consistent with the RP-HPLC analysis performed by the American Peptide Company (Fig. 2b–d).

This work characterizes the effects of PEGylation of TP508 on its plasma half-life and resulting biological activity when administered by injection. The plasma half-life of the TP508 derivatives was evaluated using fluorescent TAMRA-labeled variants of TP508 and each of the derivatives, using blood taken from CD-1 outbred mice at various timepoints after intravenous tail vein injection. The biological activity of the TP508 derivatives was then assessed in a murine model of radiation combined with injury, at an injection dose in which TP508 improves the impairment of tissue repair by approximately 50%. A complementary assay observing the angiogenic potential of aortic rings harvested from mice injected with TP508 or TP508 derivatives was used to confirm enhanced biological activity of TP508 derivatives. Finally, the effect of PEGylation on the specific activity of TP508 was assessed using an *in vitro* assay analyzing the repair of DNA double-strand breaks (DSBs) resulting from ionizing radiation using the γ-H2AX assay.

MATERIALS AND METHODS

Materials

All TP508, PEGylated TP508 derivatives, and 5-tetramethylrhodamine (5-TAMRA) fluorescently labeled TP508 and derivatives were synthesized by the American Peptide Company (Sunnyvale, CA). PEG5k-, PEG20k-, and PEG30k-TP508 derivatives were synthesized using *N*-hydroxysuccinimidyl ester (NHS)-functionalized PEGs to bind to the N-terminal amine at the end of new solid-phase peptide synthesis for site-specific N-terminal modification. PEG20k-Cys14-TP508 was synthesized using a maleimide-functionalized PEG20k to covalently bind to TP508 at the

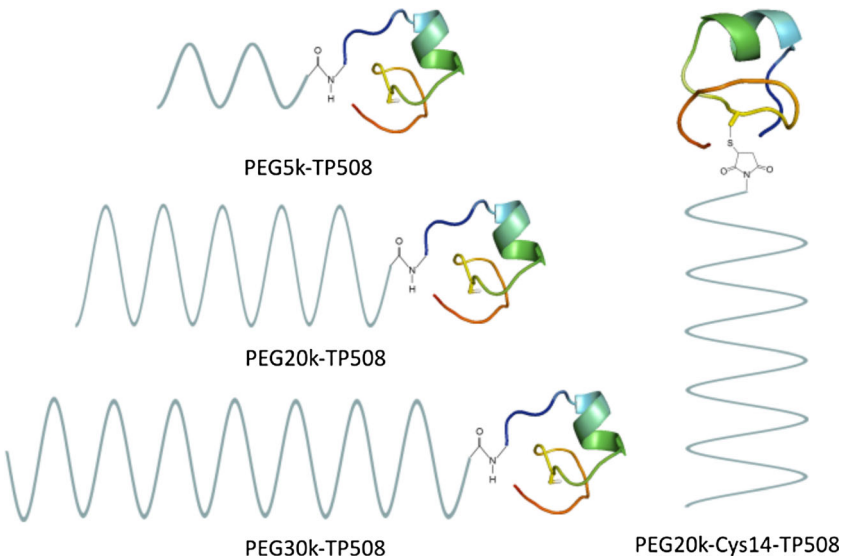

Fig. 1. TP508 derivatives PEGylated at the N-terminus or Cys14 residue

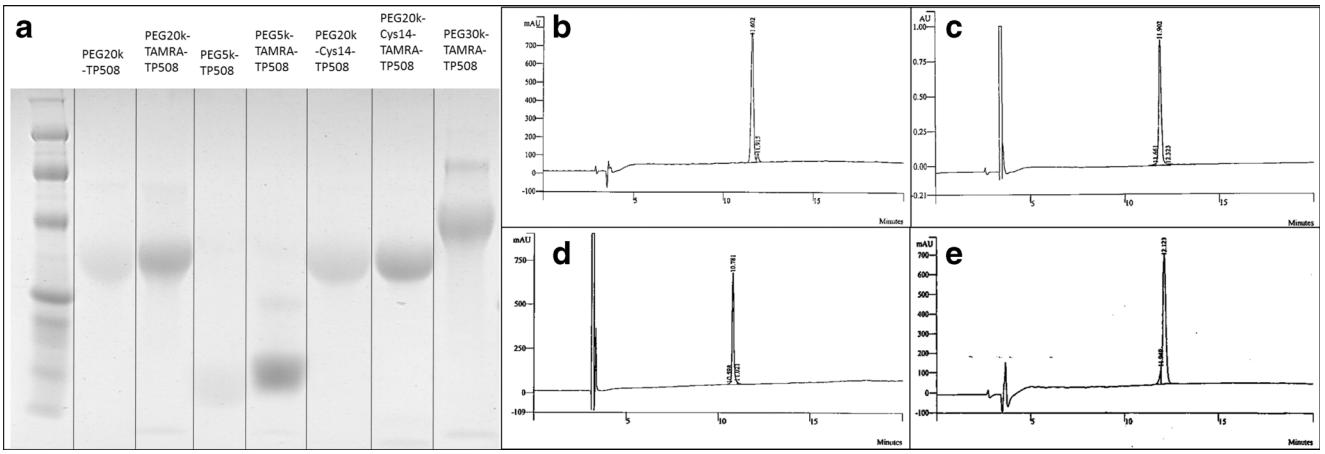

Fig. 2. Purity of synthesized TP508 derivatives. **a** SDS-PAGE of PEGylated TP508 derivatives. SDS-PAGE confirmed the specifications of ≥95% purity determined by the American Peptide Company using RP-HPLC for **b** PEG5k-TP508, **c** PEG20k-TP508, **d** PEG20k-Cys14-TP508, and **e** PEG30k-TP508

internal cysteine residue at position 14 (Cys14) of TP508. Fluorescently labeled variants of the PEGylated TP508 derivatives were prepared by fresh synthesis with the inclusion of 5-TAMRA on a 3× lysine residue spacer (Lys-Lys(5-TAMRA)-Lys) between the N-terminus of TP508 and the PEG moiety. All other reagents were purchased from Sigma-Aldrich (St. Louis, MO) unless otherwise specified.

Animal Model

All experiments were conducted at the University of Texas Medical Branch (UTMB) using an IACUC-approved protocol. CD-1 outbred 11–21-week-old male mice (Harlan Laboratories, Houston, TX) were housed, five per cage, in a controlled environment with a 12:12-h light–dark schedule, temperature of 21 ± 0.5°C and room humidity of 50 ± 20% within the Animal Research Center at UTMB. Water and chow were provided *ad libitum*. Mice were allowed to acclimate for at least 14 days prior to initiation of experiments.

SDS-PAGE

SDS-PAGE was performed using Novex 10-well 4–12% Bis-Tris gels (Thermo Fisher, Waltham, MA) loaded with 6.5 nmol of each of the modified peptides. Lane no. 1 was loaded with 5 μL Bio-Rad Kaleidoscope prestained standards (cat. no. 161-0324). Run conditions were 200 V and 120 mA for 35 min using MES buffer. Gel was stained using Fisher Scientific EZ-Run protein staining solution (cat. no. BP3620-1).

RP-HPLC

Reversed-phase HPLC was performed by the American Peptide Company. Samples were analyzed on a Supelco Discovery C18 column, 4.6 × 250 mm, 5 μm (cat. no. 504971-40; Sigma-Aldrich) using a linear gradient method of 5–95% mobile phase B in 20 min at room temperature. Mobile phase A consisted of 0.1% trifluoroacetic acid (TFA) in water and mobile phase B consisted of 0.1% TFA in acetonitrile. Injection volume was 20 μL, flow rate 1 mL/min, and wavelength 215 nm.

Plasma Half-Life

Male CD-1 mice were injected intravenously with 100 μL of either 2.16 mM of TAMRA-labeled TP508, PEG5k-TP508, PEG20k-TP508, and PEG20k-Cys14-TP508 (molar equivalent of 5 mg/mL TP508), or 0.43 mM of TAMRA-labeled PEG30k-TP508 (molar equivalent of 1 mg/mL TP508). At each timepoint, mice were euthanized and blood was collected into heparinized tubes by ventricular heart puncture. Platelet-depleted plasma was isolated by centrifugation and then measured for fluorescence alongside concentration standards prepared in the same matrix using a Biotek Synergy H1 hybrid microplate reader at an excitation wavelength of 530 nm and an emission wavelength of 590 nm. Seven independent experiments were performed, with mice ranging from 11 to 20 weeks of age. No age-dependent differences in biological half-life were observed.

Radiation Combined with Injury

Male CD-1 mice aged 14 weeks received either 8 Gy of ionizing radiation from a ^{137}Cs gamma irradiator (Mark 30, Shephard and Associates, San Fernando, CA) or sham treatment at $T = -2$ days (prewounding). On $T = -1$ day (prewounding), 10 mice per treatment group were injected intraperitoneally (i.p.) with either 100 μL of 0.9% saline (Hospira; Lake Forest, IN) or 43.4 nmol of TP508, PEG5k-TP508, PEG20k-TP508, PEG20k-C14-TP508, or PEG30k-TP508 in 100 μL of 0.9% saline. At wounding day 0, mice were anesthetized with isoflurane followed by i.p. injection of ketamine/xylazine. After clipping of dorsal fur to expose skin, mice received a full-thickness 1.2 cm × 1.2 cm dorsal excision. Day 0 wound area was imaged using a Wound Zoom camera (Wound Zoom, Inc.; Stevens Point, WI). Wounds were covered with TegaDerm transparent film dressings (3M Health Care; St. Paul, MN) to prevent detritus contamination and infection at the wound site. Mice were allowed to regain consciousness in a temperature-controlled recovery area, and received an i.p. injection of buprenorphine for pain. At

postwounding day 3, TegaDerm dressings were removed to allow clear imaging of the wound site. Wound Zoom images of each mouse were taken at days 3, 5, 7, 10, 13, and 15 postwounding. Wound areas were calculated automatically by the Wound Zoom software by using four positioning lasers on each image to determine distance of the camera from the wound in combination with user definition of the wound periphery in each image.

Aortic Ring Assay with *In Vivo* Administration

Male CD-1 mice aged 16–18 weeks were injected i.p. with 100 μL of 0.9% saline or 43.4 nmol of TP508, PEG5k-TP508, PEG20k-TP508, PEG20k-Cys14-TP508, or PEG30k-TP508 in 100 μL 0.9% saline. Twenty-hours postinjection, aortas were isolated, cleaned, sectioned, and placed into chamber slides containing Growth Factor Reduced Matrigel (Corning; Corning, NY). Explants were incubated for 7 days at 37°C, 5% CO_2, with EGM2-MV media (PromoCell, Heidelberg, Germany) changes every 2–3 days. On days 4, 5, and 6, sprouts were counted *in situ* using phase contrast microscopy.

γ-H2AX Assay

Human dermal microvascular endothelial cells (HDMECs, cat. no. C-12215; PromoCell) were cultured overnight on glass cover slips in 24-well plates at a concentration of 2.5×10^4 cells per well. On the following morning, culture media was removed and 450 μL of fresh EGM2-MV media was added to each well. Cells were then pretreated with either 50 μL of 0.9% saline solution as control or 50 μL of 10× concentrated stocks of TP508 or the PEGylated TP508 derivatives in 0.9% saline solution. Final concentration in media was 86.5 μM for TP508. PEG5k-TP508, PEG20k-TP508, PEG20k-Cys14-TP508, and PEG30k-TP508 were tested at 86.5, 434, or 1080 μM. After 1 h pretreatment, cells received 6 Gy of ionizing radiation from a ^{137}Cs gamma irradiator. At 1 and 5 h postirradiation, cells were fixed in 4% formalin and labeled with anti γ-H2AX primary antibody (cat. no. 05-636; Millipore, Billerica, MA), followed by FITC-conjugated secondary antibody (cat. no. A-11001; Life Technologies, Grand Island, NY) to identify DNA damage foci. Cover slips were counterstained with 0.1 mg/mL DAPI to identify HDMEC nuclei and mounted onto glass slides. Images were taken at ×40 objective using a Leica DMLB fluorescent microscope. Foci per nucleus were automatically counted with CellProfiler software (32,33).

RESULTS

PEGylation Increases the Plasma Half-Life of TP508 in a Size-Dependent Manner

The plasma half-life of fluorescently labeled TP508 follows a standard one-phase decay rate with a calculated plasma half-life of 13.7 min (Fig. 3, blue). This value falls within the range of 10–14 min previously reported (15). It is believed that this rapid decay rate is primarily due to renal clearance of the peptide through the kidneys. The addition of PEG5k to the N-terminus of TP508 did not extend the half-life of the molecule, with PEG5k-TP508 $t_{1/2} = 11.5$ min (Fig. 3, purple). This is as expected since the molecular weight of PEG5k-TP508 is only 7.3 kDa, well below the 20-kDa renal filtration limit of proteins. Also, the murine plasma half-life of a similar-sized PEG alone, monomethoxy PEG6000, is similar to that of TP508 at 18 min (34).

The calculated plasma half-life of PEG20k-Cys14-TP508 was $t_{1/2} = 70$ min (Fig. 3, brown), while that of PEG20k-TP508 was $t_{1/2} = 93$ min (Fig. 3, orange). These equate to 5- and 7-fold increases over the plasma half-life of TP508, respectively. Due to limited fluorescent peptide availability and solubility considerations, PEG30k-TP508 was injected at a concentration of 0.43 mM, one fifth of the amount of the other peptides. This reduction in concentration led to a greater relative error in the plasma fluorescence measurements and greater uncertainty in the calculated plasma half-life. Nevertheless, the PEG30k-TP508 plasma half-life was on the order of $t_{1/2} = 258$ min (Fig. 3, green), equivalent to a 19-fold increase over TP508.

Effect of TP508 and TP508 Derivatives on Wound Closure in a Murine Model of Radiation Combined with Injury

It is well known that radiation delays wound healing. We therefore used male CD-1 outbred mice in a model of radiation combined with injury to determine whether the extended plasma half-life of the PEGylated TP508 derivatives results in enhanced wound healing as compared to TP508 when injected systemically. CD-1 mice were chosen because they have previously been used to demonstrate radiomitigation properties of TP508 (20,21). A Wound Zoom camera, which makes use of four positioning lasers (seen as red lighting at corners of images in Figs. 4 and 5) to determine scale, was used for wound imaging, and its onboard software was used to calculate wound areas based on the user-defined periphery of each wound. To assess the effects of TP508 derivatives with increased plasma half-life on wound healing in this radiation-impaired model, a concentration of TP508 was selected based on previous studies to stimulate an approximately half-maximal increase in wound healing rate between the sham-irradiated animals and those receiving 8 Gy ionizing radiation, leaving opportunity for the TP508 derivatives to outperform TP508 at this concentration by further increasing the wound healing rate toward that of the unimpaired control. In order to dose $n = 10$ mice per treatment group within the limits of ±30 min of 24 h after irradiation, it was necessary to migrate from intravenous injection (which can take 2–5 min per mouse to dilate the tail vein with warming) to an intraperitoneal injection route.

CD-1 mice receiving a 1.2-cm × 1.2-cm full dorsal thickness wound after sham irradiation at $T = -2$ days and intraperitoneal injection of saline at $T = -1$ day display 84% wound closure by day 15 postwounding (Fig. 4, top). When these animals receive 8 Gy of ionizing radiation (Fig. 4, bottom), wound healing is greatly impaired and the mean wound closure is only 47% by day 15. The irradiated animals also display a greater degree of wound spreading from the initial square defect through day 5, resulting in more rounded wounds that are slightly larger than those of the unirradiated animals at day 3 and day 5 postwounding (ns).

PEGylation of TP508 increases plasma half-life and bioactivity

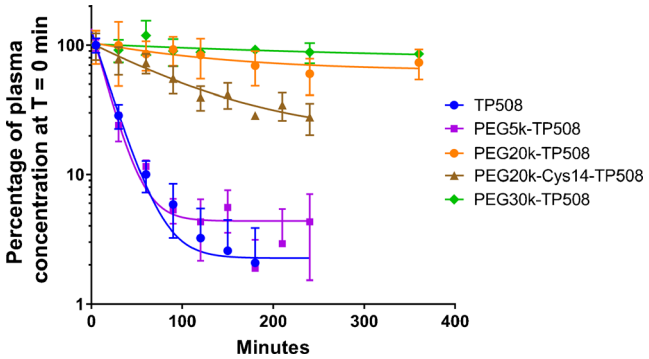

Fig. 3. Time course of TP508 and TP508 derivative concentrations in plasma after intravenous tail vein injection in male CD-1 mice. Plasma half-life analysis performed using nonlinear regression–one-phase exponential decay function in GraphPad Prism 7.01. Data presented as percentage of initial plasma concentration at $T = 0$ min. Data points represent mean ± SD at each time point ($n = 3$ mice per time point)

Representative wound areas from 8 Gy irradiated animals at day 5 and day 15 postwounding are shown in Fig. 4. At day 5, the TP508-treated animals display smaller wounds that are closer in shape to the original square defect than the 8-Gy saline control. By day 15, the mean wound area of the TP508 treatment group was 0.57 mm^2, equal to 60% wound closure. The PEG5k-TP508 treatment group increased wound closure at day 15 to 67%, while the PEG30k-TP508 treatment group reached 73% wound closure. The mean wound areas from the PEG20k-TP508 and PEG20k-Cys14-TP508 treatment groups were similar to the 8-Gy saline control, at 50 and 51% wound closure by day 15, respectively (Fig. 5).

To quantify the effects of the derivatives, we analyzed the rates of wound closure from days 3 to 15. This analysis showed that sham-irradiated animal wounds (vertical lined bar, Fig. 6) closed at a rate of 9.5 ± 0.6 mm^2/day. This rate is reduced to 6.0 ± 0.6 mm^2/day in the 8-Gy saline control group (white bar, Fig. 6), a 37% reduction in wound healing rate as compared to the sham-irradiated control. A single 43.4-nmol intraperitoneal injection of TP508 (equivalent to 100 μg or 2.5 mg/kg) administered 24 h after irradiation significantly increased the healing rate to 7.4 ± 0.6 mm^2/day ($p = 0.0043$). This represents a 40% recovery of the wound healing rate impaired by 8 Gy irradiation and results in visibly smaller wounds at both day 5 and day 15 postwounding (Fig. 6). For the PEGylated TP508 derivatives, a 43.4-nmol injection of either PEG5k-TP508 (9 ± 1 mm^2/day, $p = 0.009$) or PEG30k-TP508 (10 ± 1 mm^2/day, $p = 0.0008$) enhanced the wound healing rate to a level similar to the sham-irradiated control (Figs. 5 and 6). These results indicate that the PEGylated TP508 derivatives administered *via* i.p. injection enter circulation at sufficient concentrations to enhance wound healing in this RCI model. However, neither the PEG20k-Cys14-TP08 nor the PEG20k-TP508 treatment groups significantly increased the wound healing rate over the 8-Gy saline control group at this dose.

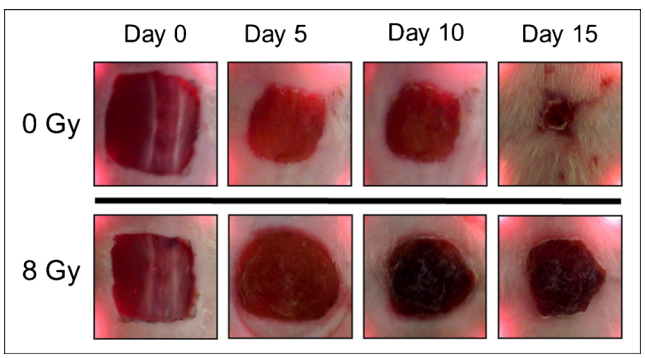

Fig. 4. Wound closure comparison between CD-1 mice with and without exposure to 8 Gy ionizing radiation. Male CD-1 mice receiving 0 Gy (*top*) or 8 Gy ionizing radiation (*bottom*) at day −2, followed with i.p. injection with 100 μL 0.9% saline at day −1 prior to receiving a 1.2-cm × 1.2-cm full dorsal excision. Representative Wound Zoom images are shown for postwounding days 0, 5, 10, and 15

In Vivo Administration of TP508 or Specific TP508 Derivatives Enhances Endothelial Sprouting in the Aortic Ring Assay

The mouse aortic ring assay is used to study growth factor, siRNA, or small molecule drug effects on angiogenic sprouting on sections of aortic tissue cultured in extracellular matrix *ex vivo* (35). Treatment of the aortic tissue traditionally occurs *in vitro* after the thoracic aorta has been isolated and prepared for culture. However, to capture the effect of increased plasma half-life that PEGylation may have on TP508 proangiogenic activity, we modified the mouse aortic ring assay by administering 43.4 nmol of TP508 or the PEGylated TP508 derivatives intraperitoneally 24 h before isolating the aortic tissue. This is the same dosage of TP508 which was selected to demonstrate efficacy in increasing the wound closure rate in the radiation combined with injury model.

Aortic explanted rings from mice aged 14–21 weeks begin to show sprouting on day 3 of incubation in Growth Factor Reduced Matrigel, with exponential growth in the number of branching sprouts occurring from days 4 to 6. On each of these days, the number of endothelial sprouts per ring was recorded manually, and by day 5, significant differences in sprouting between treatments were observed. Rings from TP508-treated animals (dark gray bars) showed a 46% increase in mean number of sprouts over saline control (white bars) on day 5 (Fig. 7a) and a 48% increase over saline control at day 6 (white bars, Fig. 7b). In comparison, aortas isolated from animals treated with the same dose of PEG5k-TP508 (hatched bars) displayed significantly enhanced angiogenesis with a 175% increase in the number of endothelial sprouts over the saline control by day 5 ($p = 0.017$,

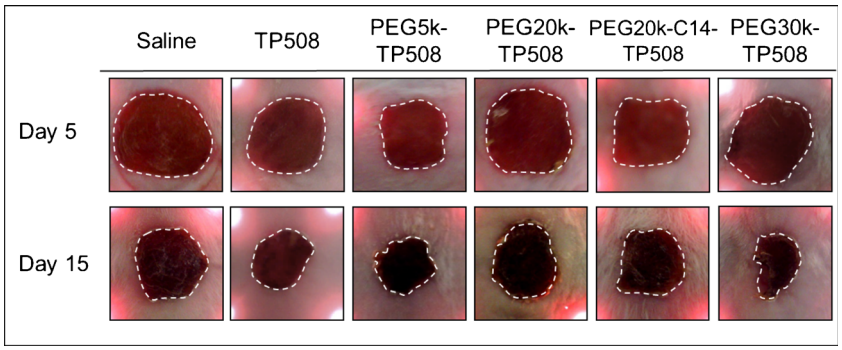

Fig. 5. Wound closure in a murine model of radiation combined with injury. Male CD-1 mice receiving 8 Gy ionizing radiation at day −2, followed with 100 μL i.p. injection of either 0.9% saline, 43.4 nmol TP508, or TP508 derivative in 0.9% saline at day −1 prior to receiving a 1.2-cm × 1.2-cm full dorsal excision. Representative images from Wound Zoom camera taken at days 5 and 15 postwounding. *Dashed white lines* represent wound periphery used by Wound Zoom software to calculate wound area

Fig. 7a) and a 160% increase in sprouting on day 6 ($p = 0.013$, Fig. 7b). The PEG30k-TP508 derivative (horizontal lined bars) also significantly enhanced endothelial sprouting, with a 180% increase in sprouting on day 5 (180% increase, Fig. 7a) and a 137% increase on day 6 ($p = 0.021$, Fig. 7b). The PEG20k-TP508 and PEG20k-Cys14-TP508 derivatives (light gray and medium gray bars, respectively) displayed levels of endothelial sprouting similar to saline control on both day 5 and day 6, indicating no proangiogenic effect at this dosage.

The γ-H2AX Assay Demonstrates Enhanced DNA Repair with TP508 Derivative Pretreatment *In Vitro*

To determine whether the PEG20k-TP508 and PEG20k-Cys14-TP508 derivatives had lost biological activity due to PEGylation or were simply at concentrations outside the therapeutic window, the derivatives were also evaluated for radioprotective activity *in vitro*. Our previous studies have shown that TP508 accelerates DNA DSB repair in irradiated HDMECs (21). Therefore, we chose to evaluate DNA repair in HDMECs using the γ-H2AX assay for quantifying the repair of DNA DSBs. Ionizing radiation resulting in DNA DSBs induces phosphorylation of histone H2AX, an isoform of histone H2A, within seconds of radiation exposure (36). Phosphorylated H2AX, also known as γ-H2AX, then localizes to DSB sites to allow for assembly of DNA repair machinery. This creates foci of γ-H2AX which can be monitored using immunofluorescence to evaluate changes in DNA DSB repair. By 5 h after 6 Gy ionizing radiation, HDMECs that have received TP508 pretreatment at a concentration of 0.2 mg/mL (86.5 μM) display a greater degree of DSB repair, indicated by a reduced number of γ-H2AX foci per nucleus (21). Since PEGylation of TP508 is anticipated to reduce the specific activity of the molecule, we screened each of the TP508 derivatives at 86.5 μM, 434 μM, and 1.08 mM (corresponding to 0.2, 1.0, and 2.5 mg/mL

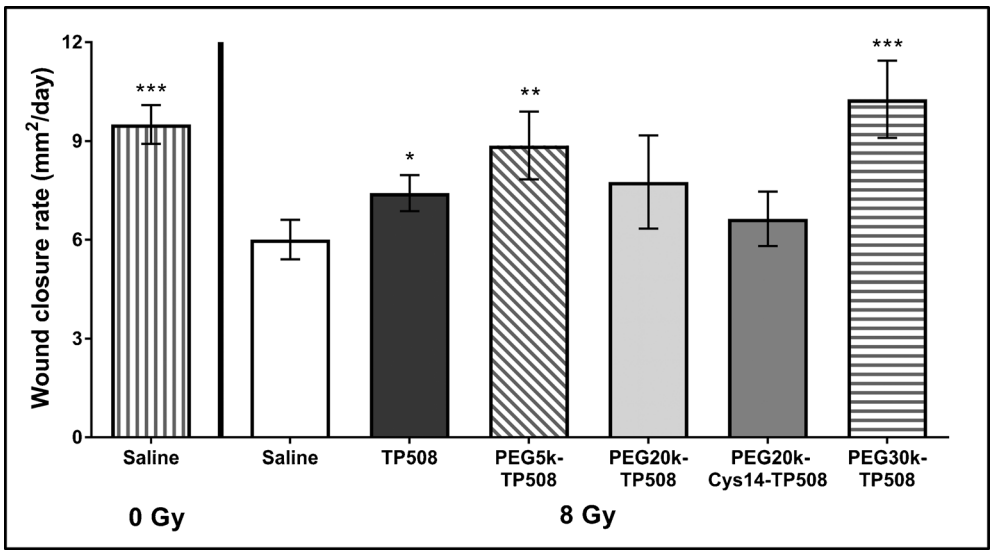

Fig. 6. Wound closure rates in a murine model of radiation combined with injury. Images from postwounding days 3–15 were used to determine wound area using Wound Zoom software. Wound closure rates were then calculated from wound area data using linear regression analysis in SigmaPlot version 12. Data presented as mean ± SD ($n = 10$ mice, $^*p < 0.05$, $^{**}p < 0.01$, $^{***}p < 0.001$ *vs* 8 Gy saline control treatment group)

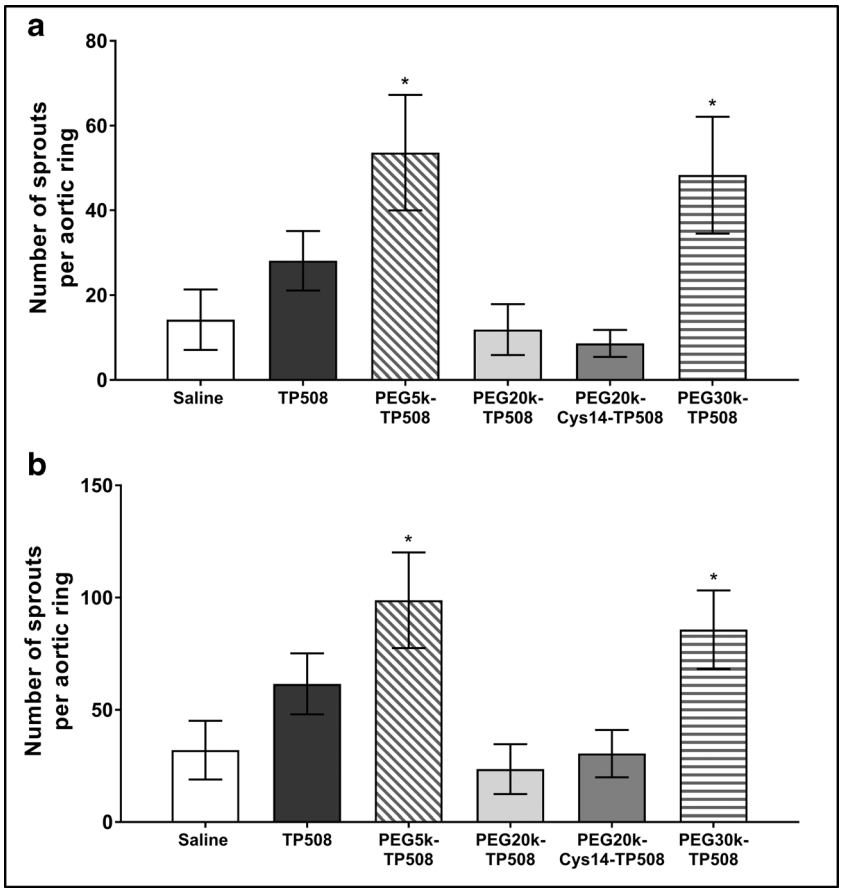

Fig. 7. Angiogenic sprouting of aortic rings after *in vivo* treatment with TP508 and TP508 derivatives. Thoracic aortas were isolated 24 h after i.p. injection of 43.4 nmol TP508 or TP508 derivatives in sterile saline or saline alone. Number of endothelial sprouts per ring counted after **a** 5 days of incubation and **b** 6 days of incubation in growth factor reduced Matrigel and EGM2-MV media. $n = 3$ mice, 8–12 explants/mouse. Data presented as mean ± SEM ($n = 3$ mice, 8–12 rings/mouse, $^*p < 0.05$ *vs* saline control)

TP508, respectively) in the same model to determine if any of these concentrations resulted in a reduction in γ-H2AX foci at 1 and 5 h postirradiation.

No significant differences in the number of γ-H2AX foci per nucleus in the irradiated HDMECs were observed at 1 h, where the saline control had a mean of 22.7 speckles per nucleus (data not shown). By 5 h, the γ-H2AX-labeled immunofluorescent images demonstrate visible reductions of foci per nucleus between the saline control and either TP508 or the TP508 derivatives (Fig. 8). At the 5-h timepoint, the saline control has reduced to 18.3 foci per nucleus (Fig. 9, white bar). This equates to a mean reduction of 4.4 foci per nucleus in HDMECs between 1 and 5 h post 6 Gy ionizing radiation. TP508 treatment at a dose of 86.5 μM significantly enhances DSB repair as compared to saline control, with a mean of 7.0 speckles per nucleus (Fig. 9, dark gray bar, $p < 0.0001$). At the same dose, PEG5k-TP508 also enhances DSB repair as compared to saline control, with a mean of 8.3 foci per nucleus (Fig. 9, hatched bar, $p < 0.0001$). At the 434-μM concentration, no significant difference from saline control was observed for TP508 or any of the TP508 derivatives. For the larger weight PEGylated TP508 derivatives, accelerated DNA damage repair is only seen at the highest concentration tested, 1.08 mM. At this concentration, PEG20k-TP508 had a mean of 11.4 foci/nucleus (Fig. 9, light gray bar, $p < 0.0001$), while PEG20k-Cys14-TP508 had a mean of 5.9 foci/nucleus (Fig. 9, medium gray bar, $p < 0.0001$) and PEG30k-TP508 had a mean of 14.4 foci/nucleus (Fig. 9, horizontal lined bar, $p = 0.009$).

DISCUSSION

A number of studies have demonstrated the potential use of TP508 as a regenerative drug for tissue repair. More recent studies show that systemic injection of TP508 mitigates the effects of myocardial ischemia (15,16,37) and radiation exposure (21,38). Because of the increasing potential for a nuclear accident or intentional detonation, a great deal of effort is being expended to determine if TP508 may be developed as a nuclear countermeasure that could be field delivered after a nuclear incident. In this scenario, TP508 administered as a single injection up to 24 h after exposure must mitigate radiation damage and delay mortality while emergency medical treatment is mobilized. Increasing the bioavailability of TP508 after systemic injection by preventing its rapid clearance through the kidney may enhance its efficacy or reduce the dosage required for effective radiomitigation. Reduced dosage requirements and the

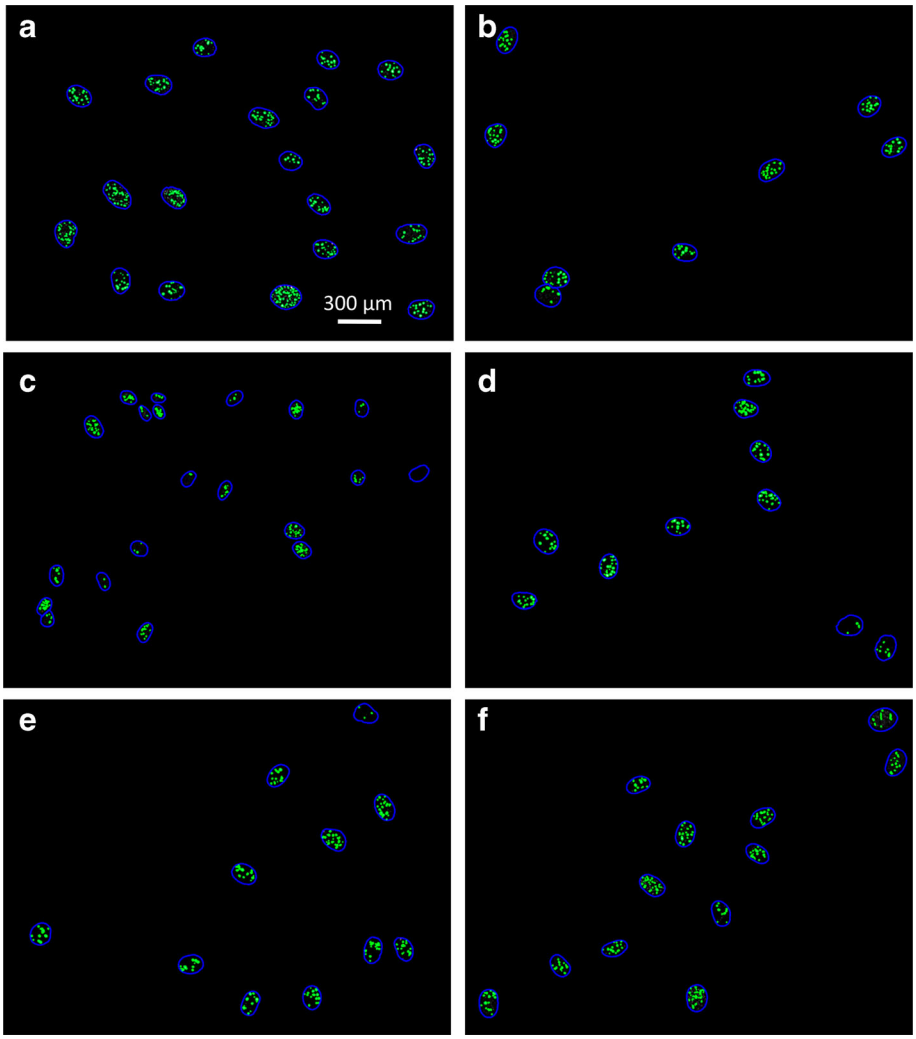

Fig. 8. Repair of DNA double-stranded breaks in HDMEC 5 h after 6 Gy ionizing radiation visualized by immunofluorescence of γ-H2AX foci. HDMECs were pretreated with the TP508 derivatives at concentrations of 86.5, 434, or 1080 µM 1 h prior to receiving 6 Gy of ionizing radiation. At 5 h postirradiation, cells were fixed with paraformaldehyde and labeled with anti-γ-H2AX antibody. Nuclei were counterstained with DAPI. Images were overlaid in CellProfiler software for automated counting of γ-H2AX foci (*green*) per nucleus (*blue outlines*). Reductions in the number of γ-H2AX foci per nucleus from **a** 0.9% saline were seen using 86.5 µM pretreatment with either **b** TP508 or **c** PEG5k-TP508; or 1080 µM of either **d** PEG20k-TP508, **e** PEG20k-Cys14-TP508, or **f** PEG30k-TP508

commensurate reduced production cost per dose would allow stockpiling of a greater number of doses in case of emergency. In addition, enhancing the radiomitigation efficacy of TP508 could save additional lives in the event of a nuclear incident. With these key goals in mind, we evaluated PEGylation of TP508 to address the issue of its short circulating half-life.

Extending the plasma half-life of therapeutic proteins prolongs their systemic availability, which can either enhance or prolong their biological activity. Covalently modifying small proteins with PEG at one or more sites greatly increases their hydrodynamic volume, reducing their elimination through the kidneys. Thus, for PEG5k-TP508, the size of the molecule is not sufficient to prevent renal elimination, but PEG20k and 30k derivatives prevent this rapid elimination and significantly extend plasma half-life. One of the trade-offs for enhanced circulating half-life of proteins due to PEGylation is a loss in their specific activity, due to factors such as steric hindrance of binding site access by the PEG, conformational changes in the protein due to PEG conjugation, and diffusion effects caused by the increased size of the molecule (39,40). Thus, for PEGylation of TP508 to successfully enhance biological activity *in vivo*, the contribution of increased biological half-life must outweigh any loss of specific activity.

Plasma half-life analysis of the PEGylated TP508 derivatives confirmed that the plasma half-life of TP508 increased as the size of the covalently attached PEG increased. The increased hydrodynamic volume of PEG5k-TP508 was insufficient to increase plasma half-life. Attachment of PEG20k to the internal cysteine residue resulted in a 5-fold increase in plasma half-life. When PEG20k was attached to the N-terminus of TP508, it resulted in a 6-fold increase in plasma half-life over TP508. PEG30k-TP508 had the greatest effect

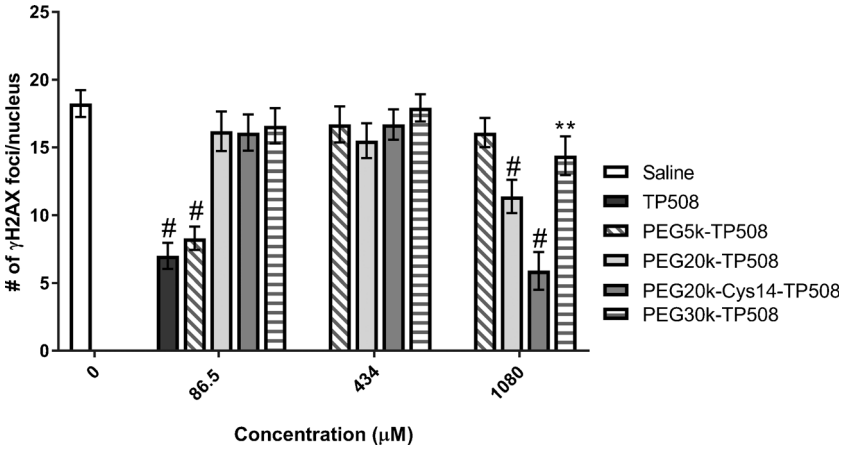

Fig. 9. Dose-dependent effect of *in vitro* TP508 derivative treatment on DNA repair in HDMECs 5 h after 6 Gy ionizing radiation. Data presented as mean ± 95% confidence interval ($n \leq 128$ cells per treatment, $^{**}p < 0.01$, $\#p < 0.0001$ *vs* saline control)

on plasma half-life, on the close order of 19-fold, which increases the plasma half-life of TP508 from less than 15 min to over 4 h.

A combination of *in vivo* assays using systemic injection to determine whether the increased circulating half-life of PEGylated TP508 derivatives correlates with enhanced bioactivity was used to assess their tissue repair effects with and without radiation. For these assays, we selected a single molar concentration for comparison of the PEGylated TP508 derivatives to monomeric TP508. At the chosen concentration, TP508 produced a roughly half-maximal stimulation of angiogenesis and wound healing, allowing the TP508 derivatives to demonstrate improvements in tissue repair over TP508. Our study design also incorporated an established *in vitro* assay of DNA repair using the γ-H2AX assay to quantify DNA double-strand breaks to determine the extent of reduction in specific activity of the TP508 derivatives compared to TP508, and to verify that they all retained some level of radioprotective activity.

The first *in vivo* assay, a murine model of radiation combined with injury, was used to evaluate the ability of PEGylated TP508 derivatives to enhance tissue repair after radiation exposure. Impairment of cutaneous wound healing shortly after ionizing radiation has been well characterized due to its relevance to surgical procedures performed following radiation therapy (41). Acute effects of ionizing radiation leading to the impairment of wound healing include reduced fibroblast proliferation and collagen formation (42,43), delayed resolution of inflammation (44), and impaired revascularization of the wound (45). This leads to a greater susceptibility to infection and less complete healing. TP508 has been shown to help combat these impairments in other models of impaired wound healing, including ischemic wounds (8) and diabetic foot ulcers (10,19), leading to the hypothesis that TP508 would improve healing in radiation combined with injury.

This study confirmed that a single 100 μg i.p. injection of TP508 (43.4 nmol) increases the wound healing rate of CD-1 mice receiving 8 Gy of ionizing radiation approximately 25% over placebo. Intraperitoneal injections at the same molar concentration of PEG5k-TP508 and PEG30k-TP508 increased the wound healing rate by 50 and 67% over placebo, respectively. In contrast, both the PEG20k-TP508 and PEG20k-Cys14-TP508 were ineffective in stimulating wound closure. Thus, the biological activity results did not simply correlate with increased plasma half-life, since PEG5k-TP508 enhanced healing over TP508 despite having a similar half-life, and both TP508 derivatives attached to PEG20k had no activity despite having a 5–6-fold increase in plasma half-life over TP508.

To confirm the wound healing results, we also evaluated the effects of TP508 and the TP508 derivatives using a modified version of the mouse aortic ring assay (35). In this assay, TP508 or TP508 derivatives were injected intraperitoneally into naive male CD-1 mice and their aortas isolated 24 h later for culture *ex vivo*. This assay has the advantage of not relying on the complexities of radiation-impaired wound healing and reduces the time period necessary to evaluate the biological efficacy of TP508 and the derivatives.

Results for TP508 derivative administration *in vivo* are consistent between the aortic ring model of angiogenesis and the radiation combined with injury model, with PEG5k-TP508 and PEG30k-TP508 enhancing angiogenesis and wound healing, while PEG20k-TP508 and PEG20k-Cys14-TP508 did not demonstrate any significant effects. In the case of the PEG20k-Cys14-TP508 derivative, where PEGylation occurs central to the polypeptide sequence of TP508, it was possible that PEGylation at this location completely abolishes activity due to steric hindrance of the TP508 active site in binding to its cellular receptor, or prevents TP508 from adopting a conformation necessary for receptor binding. However, this does not explain the loss of *in vivo* activity for the PEG20k-TP508 derivative, where PEGylation occurs at the same location as the PEG5k-TP508 and PEG30k-TP508.

Using the DNA repair γ-H2AX *in vitro* assay, we observed a significant reduction in γ-H2AX foci per nucleus at 5 h with TP508 treatment of HDMECs at a concentration of 86.5 μM (equivalent to 0.2 mg/mL TP508), as was previously reported (21). This reduction demonstrates that TP508 accelerates DNA double-strand break repair in these cells. PEG5k-TP508 showed similar results when administered at the same concentration. At higher concentrations, however, the TP508 and PEG5k-TP508 treatment effects on

DNA repair in HDMECs were not significantly different from saline control. This recapitulates previous *in vivo* observations that there is a reduction in TP508 efficacy above a certain therapeutic window (14,21). PEG30k-TP508 demonstrated a small but significant amount of DNA repair acceleration, but only at the 1080-μM concentration, 12.5× higher than the effective concentration of TP508 and PEG5k-TP508. PEG20k-TP508 and PEG20k-Cys14-TP508 also showed radioprotective acceleration of DNA repair in HDMECs only at the 1080-μM concentration. These results may suggest that the 5–6-fold extension of biological half-life for PEG20k-TP508 and PEG20k-Cys14-TP508 is insufficient to overcome the loss of specific activity caused by PEG20k attachment, while the PEG30k-TP508 compound, with its much longer plasma half-life, retains *in vivo* activity despite its loss of specific activity *in vitro*. However, it should be noted that the *in vivo* assays were performed using i.p. injection, while plasma half-life was determined using i.v. injection. The increased hydrodynamic volume as PEG size increases may slow tissue diffusion through the peritoneal cavity, adding an additional factor to the resulting biological activity. The plasma concentration of the PEGylated TP508 derivatives using alternate routes of administration may be assessed in future experiments once an optimal route of administration for TP508 in radiomitigation applications has been identified.

CONCLUSIONS

PEGylation of TP508 increased the plasma half-life of the TP508 derivatives in a size-dependent manner although biological activity did not simply correlate with increased half-life. The PEG20k-TP508 and PEG20k-Cys14-TP508 derivatives showed a 5–6-fold enhancement in plasma half-life but did not demonstrate *in vivo* activity when administered i.p. at concentrations equimolar to TP508. PEG5k-TP508 displayed enhanced *in vivo* activity over TP508 using i.p. injection, despite having the same plasma half-life. PEG30k-TP508 increased plasma half-life on the order of 19-fold and also enhanced *in vivo* biological activity using i.p. injection. This work identifies PEG5k-TP508 and PEG30k-TP508 as potential second-generation TP508 molecules for drug development.

ACKNOWLEDGMENTS

The authors would like to acknowledge Dr. Gerald M. Fuller (University of Alabama) and Dr. Laurie M. Sower (Chrysalis BioTherapeutics, Inc.) for their encouragement during this project and editorial assistance; Dr. Kimberly Burckart and Dr. Barbara Olszewska-Pazdrak, members of the Carney Laboratory, and Dr. Bradford Loucas, at the University of Texas Medical Branch, for assistance with animal studies. This work was supported by NIH/NIAID Grant 5R44AI086135.

COMPLIANCE WITH ETHICAL STANDARDS

Conflict of Interest Chrysalis BioTherapeutics has licensed worldwide exclusive rights to TP508 from The University of Texas Medical Branch. DHC and KR receive compensation from Chrysalis BioTherapeutics or have stock or stock options in the company. Potential conflicts of interest are managed by the University of Texas Medical Branch Conflicts of Interest and Commitment Committee.

REFERENCES

1. Glenn KC, Frost GH, Bergmann JS, Carney DH. Synthetic peptides bind to high-affinity thrombin receptors and modulate thrombin mitogenesis. Pept Res. 1988;1(2):65–73.
2. Norfleet AM, Bergmann JS, Carney DH. Thrombin peptide, TP508, stimulates angiogenic responses in animal models of dermal wound healing, in chick chorioallantoic membranes, and in cultured human aortic and microvascular endothelial cells. Gen Pharmacol. 2000;35(5):249–54.
3. Vartanian KB, Chen HY, Kennedy J, Beck SK, Ryaby JT, Wang H, *et al*. The non-proteolytically active thrombin peptide TP508 stimulates angiogenic sprouting. J Cell Physiol. 2006;206(1):175–80.
4. Wang Y, Wan C, Szöke G, Ryaby JT, Li G. Local injection of thrombin-related peptide (TP508) in PPF/PLGA microparticles-enhanced bone formation during distraction osteogenesis. J Orthop Res. 2008;26(4):539–46.
5. Olszewska-Pazdrak B, Hart-Vantassell A, Carney DH. Thrombin peptide TP508 stimulates rapid nitric oxide production in human endothelial cells. J Vasc Res. 2010;47(3):203–13.
6. Freyberg S, Song YH, Muehlberg F, Alt E. Thrombin peptide (TP508) promotes adipose tissue-derived stem cell proliferation via PI3 kinase/Akt pathway. J Vasc Res. 2009;46(2):98–102.
7. Pernia SD, Berry DL, Redin WR, Carney DH. A synthetic peptide representing the thrombin receptor-binding domain enhances wound closure in vivo. SAAS Bull Biochem Biotechnol. 1990;3:8–12.
8. Norfleet AM, Huang Y, Sower LE, Redin WR, Fritz RR, Carney DH. Thrombin peptide TP508 accelerates closure of dermal excisions in animal tissue with surgically induced ischemia. Wound Repair Regen. 2000;8(6):517–29.
9. Ryaby JT, Sheller MR, Levine BP, Bramlet DG, Ladd AL, Carney DH. Thrombin peptide TP508 stimulates cellular events leading to angiogenesis, revascularization, and repair of dermal and musculoskeletal tissues. J Bone Joint Surg Am. 2006;88 Suppl 3:132–9.
10. Carney DH, Olszewska-Pazdrak B. Could rusalatide acetate be the future drug of choice for diabetic foot ulcers and fracture repair? Expert Opin Pharmacother. 2008;9(15):2717–26.
11. Wang H, Li X, Tomin E, Doty SB, Lane JM, Carney DH, *et al*. Thrombin peptide (TP508) promotes fracture repair by up-regulating inflammatory mediators, early growth factors, and increasing angiogenesis. J Orthop Res. 2005;23(3):671–9.
12. Hanratty BM, Ryaby JT, Pan XH, Li G. Thrombin related peptide TP508 promoted fracture repair in a mouse high energy fracture model. J Orthop Surg Res. 2009;4:1.
13. Li X, Wang H, Touma E, Qi Y, Rousseau E, Quigg RJ, *et al*. TP508 accelerates fracture repair by promoting cell growth over cell death. Biochem Biophys Res Commun. 2007;364(1):187–93.
14. Oyamada S, Osipov R, Bianchi C, Robich MP, Feng J, Liu Y, *et al*. Effect of dimerized thrombin fragment TP508 on acute myocardial ischemia reperfusion injury in hypercholesterolemic swine. J Pharmacol Exp Ther. 2010;334(2):449–59.
15. Chu LM, Osipov RM, Robich MP, Feng J, Sheller MR, Sellke FW. Effect of thrombin fragment (TP508) on myocardial ischemia reperfusion injury in a model of type 1 diabetes mellitus. Circulation. 2010;122(11 Suppl):S162–9.
16. Osipov RM, Bianchi C, Clements RT, Feng J, Liu Y, Xu SH, *et al*. Thrombin fragment (TP508) decreases myocardial infarction and apoptosis after ischemia reperfusion injury. Ann Thorac Surg. 2009;87(3):786–93.

17. Fossum TW, Olszewska-Pazdrak B, Mertens MM, Makarski LA, Miller MW, Hein TW, *et al*. TP508 (Chrysalin) reverses endothelial dysfunction and increases perfusion and myocardial function in hearts with chronic ischemia. J Cardiovasc Pharmacol Ther. 2008;13(3):214–25.
18. Papareddy P, Rydengård V, Pasupuleti M, Walse B, Mörgelin M, Chalupka A, *et al*. Proteolysis of human thrombin generates novel host defense peptides. PLoS Pathog. 2010;6(4), e1000857.
19. Fife C, Mader JT, Stone J, Brill L, Satterfield K, Norfleet A, *et al*. Thrombin peptide Chrysalin stimulates healing of diabetic foot ulcers in a placebo-controlled phase I/II study. Wound Repair Regen. 2007;15(1):23–34.
20. Kantara C, Moya SM, Houchen CW, Umar S, Ullrich RL, Singh P, *et al*. Novel regenerative peptide TP508 mitigates radiation-induced gastrointestinal damage by activating stem cells and preserving crypt integrity. Lab Investig. 2015;95(11):1222–33.
21. Olszewska-Pazdrak B, McVicar SD, Rayavara K, Moya SM, Kantara C, Gammarano C, *et al*. Nuclear countermeasure activity of TP508 linked to restoration of endothelial function and acceleration of DNA repair. Radiat Res. 2016.
22. Prasanna PG, Narayanan D, Hallett K, Bernhard EJ, Ahmed MM, Evans G, *et al*. Radioprotectors and radiomitigators for improving radiation therapy: the small business innovation research (SBIR) gateway for accelerating clinical translation. Radiat Res. 2015;184(3):235–48.
23. Singh VK, Newman VL, Romaine PL, Wise SY, Seed TM. Radiation countermeasure agents: an update (2011–2014). Expert Opin Ther Pat. 2014;24(11):1229–55.
24. Li P, Roller PP. Cyclization strategies in peptide derived drug design. Curr Top Med Chem. 2002;2(3):325–41.
25. Conibear AC, Chaousis S, Durek T, Rosengren KJ, Craik DJ, Schroeder CI. Approaches to the stabilization of bioactive epitopes by grafting and peptide cyclization. Biopolymers. 2016;106(1):89–100.
26. Berguig GY, Convertine AJ, Frayo S, Kern HB, Procko E, Roy D, *et al*. Intracellular delivery system for antibody-peptide drug conjugates. Mol Ther. 2015;23(5):907–17.
27. Gentilucci L. New trends in the development of opioid peptide analogues as advanced remedies for pain relief. Curr Top Med Chem. 2004;4(1):19–38.
28. Caliceti P, Veronese FM, Jonak Z. Immunogenic and tolerogenic properties of monomethoxypoly(ethylene glycol) conjugated proteins. Farmaco. 1999;54(7):430–7.
29. Lee SH, Lee S, Youn YS, Na DH, Chae SY, Byun Y, *et al*. Synthesis, characterization, and pharmacokinetic studies of PEGylated glucagon-like peptide-1. Bioconjug Chem. 2005;16(2):377–82.
30. Meyers FJ, Paradise C, Scudder SA, Goodman G, Konrad M. A phase I study including pharmacokinetics of polyethylene glycol conjugated interleukin-2. Clin Pharmacol Ther. 1991;49(3):307–13.
31. Thanou M, Duncan R. Polymer-protein and polymer-drug conjugates in cancer therapy. Curr Opin Investig Drugs. 2003;4(6):701–9.
32. Carpenter AE, Jones TR, Lamprecht MR, Clarke C, Kang IH, Friman O, *et al*. CellProfiler: image analysis software for identifying and quantifying cell phenotypes. Genome Biol. 2006;7(10):R100.
33. González JE, Lee M, Barquinero JF, Valente M, Roch-Lefèvre S, García O. Quantitative image analysis of gamma-H2AX foci induced by ionizing radiation applying open source programs. Anal Quant Cytol Histol. 2012;34(2):66–71.
34. Yamaoka T, Tabata Y, Ikada Y. Distribution and tissue uptake of poly(ethylene glycol) with different molecular weights after intravenous administration to mice. J Pharm Sci. 1994;83(4):601–6.
35. Baker M, Robinson SD, Lechertier T, Barber PR, Tavora B, D'Amico G, *et al*. Use of the mouse aortic ring assay to study angiogenesis. Nat Protoc. 2012;7(1):89–104.
36. Rogakou EP, Pilch DR, Orr AH, Ivanova VS, Bonner WM. DNA double-stranded breaks induce histone H2AX phosphorylation on serine 139. J Biol Chem. 1998;273(10):5858–68.
37. Osipov RM, Robich MP, Feng J, Clements RT, Liu Y, Glazer HP, *et al*. Effect of thrombin fragment (TP508) on myocardial ischemia-reperfusion injury in hypercholesterolemic pigs. J Appl Physiol. 2009;106(6):1993–2001.
38. Kantara C, Moya SM, Houchen CW, Umar S, Ullrich RL, Singh P, *et al*. Novel regenerative peptide TP508 mitigates radiation-induced gastrointestinal damage by activating stem cells and preserving crypt integrity. Lab Investig. 2015;95(11):1222–33.
39. Caliceti P, Veronese FM. Pharmacokinetic and biodistribution properties of poly(ethylene glycol)-protein conjugates. Adv Drug Deliv Rev. 2003;55(10):1261–77.
40. Harris JM, Chess RB. Effect of pegylation on pharmaceuticals. Nat Rev Drug Discov. 2003;2(3):214–21.
41. Wang J, Boerma M, Fu Q, Hauer-Jensen M. Radiation responses in skin and connective tissues: effect on wound healing and surgical outcome. Hernia. 2006;10(6):502–6.
42. Rudolph R, Vande Berg J, Schneider JA, Fisher JC, Poolman WL. Slowed growth of cultured fibroblasts from human radiation wounds. Plast Reconstr Surg. 1988;82(4):669–77.
43. Qu JF, Cheng TM, Xu LS, Shi CM, Ran XZ. Effects of total body irradiation injury on the participation of dermal fibroblasts in tissue repair. Sheng Li Xue Bao. 2002;54(5):395–9.
44. Denham JW, Hauer-Jensen M. The radiotherapeutic injury—a complex 'wound'. Radiother Oncol. 2002;63(2):129–45.
45. Tibbs MK. Wound healing following radiation therapy: a review. Radiother Oncol. 1997;42(2):99–106.